

# RSC Advances



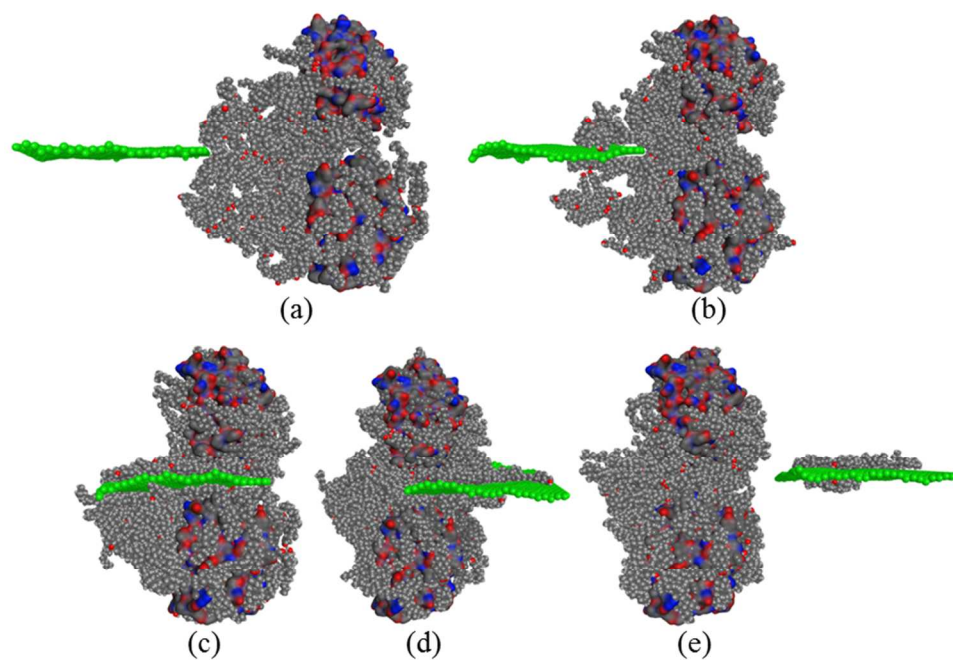
This is an *Accepted Manuscript*, which has been through the Royal Society of Chemistry peer review process and has been accepted for publication.

*Accepted Manuscripts* are published online shortly after acceptance, before technical editing, formatting and proof reading. Using this free service, authors can make their results available to the community, in citable form, before we publish the edited article. This *Accepted Manuscript* will be replaced by the edited, formatted and paginated article as soon as this is available.

You can find more information about *Accepted Manuscripts* in the [Information for Authors](#).

Please note that technical editing may introduce minor changes to the text and/or graphics, which may alter content. The journal's standard [Terms & Conditions](#) and the [Ethical guidelines](#) still apply. In no event shall the Royal Society of Chemistry be held responsible for any errors or omissions in this *Accepted Manuscript* or any consequences arising from the use of any information it contains.

## Mechanisms of Graphyne-enabled Cholesterol Extraction from Protein Clusters



Functionalized graphyne provides a novel vehicle for cholesterol removal from protein clusters by molecular dynamics simulations.

## Mechanisms of Graphyne-enabled Cholesterol Extraction from Protein Clusters

Liuyang Zhang and Xianqiao Wang\*

College of Engineering and NanoSEC, University of Georgia, Athens, GA 30602, USA

### Abstract

The health risk associated with high cholesterol levels in the human body has motivated intensive efforts to lower them by using specialized drugs. However, little research has been performed utilizing nanomaterials to remove extra cholesterol from living tissues. Graphyne, a 2D lattice of  $sp^2$ - and  $sp^1$ -hybridized carbons similar to graphene, possesses great potential for cholesterol extraction from cell membranes due to its distinct porous structure and outstanding surface adhesion. Here we employ molecular dynamics simulations to explore pathways for cholesterol removal from protein clusters by using graphyne as a promising vehicle. We first demonstrate the adhesive strength between a single cholesterol molecule and different types of pristine graphyne, which provides the foundation for the graphyne-cholesterol interaction and the dynamic cholesterol removal process within a protein cluster. The  $sp^1$ -hybridized carbons in graphynes are potentially more reactive than the  $sp^2$ -hybridized carbons in graphene, which bestows graphynes with a remarkable affinity for cholesterol molecules. Simulation results show that graphynes with more  $sp^1$ -hybridized carbon linkers can extract more cholesterol molecules than those with fewer linkers. The movement rate of graphyne across the protein cluster also plays an important role in determining the amount of removed cholesterol molecules from the system of interest. The hybrid structure of graphyne with cholesterol molecules in its partial pores also possesses outstanding adhesive strength, showing better cholesterol removal

---

\* Corresponding authors, Tel: 706-5426251; Email: [xqwang@uga.edu](mailto:xqwang@uga.edu)

performance than pristine graphyne. These findings open up a promising avenue to exploit the capability of graphyne for biomedical applications.

**Keywords: MD simulation, Cholesterol, Protein, Graphyne**

## **Introduction**

Cholesterol is a major sterol component of mammalian cell membranes which plays an important role in maintaining the physical and mechanical properties of the membrane.<sup>1-4</sup> Recently, as nanotechnology advances cholesterol has been found to be an indispensable ingredient for a variety of biological processes such as signal transduction,<sup>5</sup> protein stabilization,<sup>6</sup> protein and lipid sorting,<sup>7</sup> membrane fusion,<sup>8, 9</sup> the condensing effect,<sup>10</sup> and thermal concentration.<sup>11</sup> However, excessive cholesterol in the bloodstream leads to disastrous health issues such as cardiovascular disease and premature death.<sup>12</sup> High cholesterol concentration can trigger damage of the endothelial tissue layer (see Figure 1) by developing a fatty plaque protruding into the lumen of the artery and reducing blood flow speed in the artery. Unhealthy endothelial tissue poses great threats on human health, being the leading cause of many diseases such as hypertension, atherosclerosis, arterial plaque and heart failure.<sup>13-18</sup> Therefore, there is a critical need for developing useful techniques to remove extra cholesterol in the endothelial tissue layer and lower the associated health risks.

Recent years have witnessed the explosive growth of interests in investigating functionalized nanomaterials to ameliorate the health risks associated with high cholesterol concentration in blood vessels. For instances, a nanoparticle surrounded by a lipid shell has shown the ability to sequester cholesterol and remove it from circulation.<sup>19</sup> Nanosized particles with large surface area (poly HEMA–MAT and poly HEMA–MAP) have been synthesized and performed suitably as carriers for the adsorption of cholesterol from a medium.<sup>20</sup> Via the incorporation of

cholesterol into the cellular membrane and conversion of the cholesterol into coprostanol, probiotics have enjoyed the significant popularity in cholesterol removal.<sup>21</sup> Cholesterol extraction by electroporated cells has been attributed to the formation of pores upon electroporation that enhance membrane permeability towards cholesterol.<sup>22</sup> By employing molecular dynamics simulation,  $\beta$ -cyclodextrin has been shown to extract the cholesterol from a lipid membrane model.<sup>23,24</sup> Hydrophobic carbon allotropes, for instance carbon nanotubes, have also been demonstrated to remove cholesterol lodgment from membrane and protein surfaces.<sup>25</sup> However, from a computational viewpoint, the investigation of cholesterol removal by two-dimensional nanomaterials such as graphene is still lacking, and the fundamental mechanism of the removal process with atomic resolution remains elusive and worthy of exploration.

Carbon-based layered materials, such as graphene, because of their high specific surface area and their exceptional physicochemical properties show great promise for applications in biotechnology and biomedicine such as nanobiocatalytic systems,<sup>26</sup> gene and drug delivery,<sup>27-30</sup> bioimaging, and biosensing.<sup>31</sup> It has been demonstrated that graphene microsheets can enter cells through spontaneous membrane penetration at edge asperities and corner sites.<sup>32</sup> The antibacterial graphene and graphene oxide nanosheets<sup>33,34</sup> have shown the capability to induce the degradation of the inner and outer cell membrane of *Escherichia coli* and subsequently reduce viability.<sup>35</sup> However, graphene is not the only all-carbon 2-D material of interest; a class of materials called ‘graphynes’ have recently been synthesized<sup>36,37</sup> and are making an impact due to their promising properties as well.<sup>38,39</sup> Graphynes are a family of 2-D materials composed entirely of carbon similar to graphene; but whereas all of the atoms in graphene are  $sp^2$ -hybridized with three neighbors apiece, graphynes all contain a percentage of  $sp^1$ -hybridized acetylenic linkers, with the percentage and distribution of linkers defining the type of graphyne.<sup>38</sup>

The inclusion of single and triple bonds and an enlarged lattice gives graphynes markedly different properties when compared with pristine graphene, opening new avenues and giving new alternatives to conventional energy storage,<sup>40</sup> electronics,<sup>41-43</sup> bulk composites<sup>44</sup> and filtration technologies.<sup>45, 46</sup> Despite extensive literature on the study of graphyne, its medical application is still in a stage of infancy. Graphyne has been suggested as a conceptually new family of carbon materials that have physical properties comparable to those of graphene and chemical properties superior to those of graphene. The graphyne are expected to be better suited to biomedical applications. The functionalization via chemical substitution reactions occurring at C(*sp*)-C(*sp*) bonds on graphyne could yields superior electric conductivity and aqueous solubility than graphene.<sup>47</sup> To demonstrate our idea to remove the cholesterol molecules from the endothelium with graphyne, the extracellular domain protein 1LQV appearing in the endothelium will be chosen (see the Protein Data Bank, <http://www.rcsb.org/>). Here we will utilize molecular dynamics simulation to investigate the mechanism for removing cholesterol molecules from a 1LQV protein-cholesterol cluster (PCC) by pulling a graphyne sheet across the cluster. The graphynes to be used in this work are all  $\gamma$ -graphynes; labeled here as *N*-graphyne where *N* is the number of acetylenic linkers between hexagonal cells, varied here from 0 to 2 with 0-graphyne referring to graphene (for ease of notation). We will begin our study with the investigation of the adhesive interaction of a single cholesterol molecule on the surface of different types of graphyne as well as the energy barrier of a cholesterol molecule passing through the pore on the graphyne sheet. Then we will discuss the efficiency of cholesterol removal from the cluster with different graphyne types, pulling rates, and hybridized degree. Finally we will conclude our findings with the potential impact of our proposed cholesterol removal on the medical applications.

## Computational Model and Methodology

In the molecular dynamics (MD) simulation, we adopt the powerful CHARMM27 force field<sup>48,49</sup> to describe the bonded and non-bonded interactions between atoms. The potential components described in the CHARMM27 force field with specific parameters<sup>50</sup> are defined as

$$E_{total} = E_{bonds} + E_{angle} + E_{dihedral} + E_{impropers} + E_{Urey-Bradley} + E_{vdW} + E_{elec} \quad (1)$$

where the first five terms account for the intramolecular interactions (bond stretch, bond angle, dihedral angle, improper angle, Urey-Bradley) characterizing the short-range bonding while the last two terms are associated with intermolecular interactions describing the long-range van der Waals (vdW) interactions and electrostatic interactions. For protein, all parameters are based on from the popular CHARMM force field.<sup>51</sup> For the cholesterol molecule, the electrostatic charges for each atom are derived from the quantum mechanical molecular electrostatic potential.<sup>52</sup> The charges of the cholesterol head are distributed with -0.68 electron charges on the oxygen, +0.4 on the hydrogen, and +0.2 on the carbon to which the hydroxyl group is attached. Typically, the 12-6 Lennard-Jones potential is adopted to describe the vdW interaction based on the Lorentz-Berhelot mixing rule.

$$E_{LJ} = 4\epsilon \left[ \left( \frac{\sigma}{r} \right)^{12} - \left( \frac{\sigma}{r} \right)^6 \right] \quad (2)$$

where  $\epsilon$  is the depth of potential well,  $\sigma$  is the finite distance where the potential is zero, and  $r$  is the distance between the particles. The global cutoff for the LJ term is set here to be 10Å as a good balance between computational speed and accuracy. The Polak-Ribière conjugate gradient algorithm has been employed to perform energy minimization until the total energy change between two successive iterations divided by the energy magnitude is less than or equal to 10<sup>-8</sup> kcal/mol. After an equilibrium state is achieved, NVT ensemble simulations with a constant

temperature of 310 K are carried out based on the Berendsen thermostat.<sup>53</sup> The velocity Verlet method is utilized with an integration time step of 0.5fs.

Initially, the rectangular ( $65.4\text{\AA} \times 60.3\text{\AA}$ )  $N$ -graphyne ( $N=0, 1, 2$ ) sheets are created correspondingly as shown in Figure 2. The open carbon edges of graphyne are not chemically stable in an ambient environment, so they are terminated by covalently bonded hydrogen atoms.

We define the carbon occupancy density  $\rho = \frac{\text{Number of Carbon Atoms}}{\text{Surface area}}$ . Here,  $\rho$  is 40.6%, 31.3%,

and 25.9%, which corresponds to 0, 1, 2-graphyne. The aromatic rings in graphyne are highlighted in green to distinguish its unique structure. It should be noticed that 2-graphyne has a longer linker chain which makes it easier to bend out of plane.<sup>44</sup> The PCC structure shown in Figure 3 is obtained based on the final configuration of three 1LQV proteins together with a cholesterol pool (228 cholesterol molecules) after an energy minimization process with a duration of 100 ps. The cholesterol molecules closely adhere to the outside surface of the folded protein which implies the strong binding interaction between the cholesterol molecules and protein and ensure the integrity of the tertiary structure of proteins. The graphyne sheet is initially placed on one side of the PCC and is intended to remove cholesterol molecules in the presence of 1LQV after slowly passing through the PCC. To better demonstrate the efficiency of the cholesterol removal capability of graphyne from a protein cluster, the majority of the cholesterol molecules in the model are situated on the same side as the graphyne sheet at the beginning of the simulation. The reason is that the cholesterol molecules on the end of the pulling path have a high possibility of being pulled out from the system and should be excluded for better illustration. All simulations are performed in the GB/SA implicit water environment<sup>54</sup> and under the velocity of pulling graphyne as  $0.5 \text{ \AA/ps}$  unless otherwise stated. The cholesterol molecules around the protein are constrained to keep the protein in the confined space, able to

move around but unable to be pulled out from the system. In what follows, we will study cholesterol removal via different graphyne platforms and pulling rates as well as the hybrid structure of graphynes with cholesterol decoration in the pores.

## Results and Discussions

### Binding interaction between *N*-graphyne and a single cholesterol molecule

To better integrate graphyne into functional devices for cholesterol extraction, it is essential to understand the intermolecular adhesion between graphyne and a single cholesterol molecule. The adhesive interaction is attributed to the vdW interactions between graphyne and cholesterol, however, the fundamental understanding of binding interaction between graphene and cholesterol with a quantitative calibration remains poorly exploited. Therefore, we design a set of simulations to unravel the possibility of using *N*-graphyne to capture cholesterol molecules from the PCC. A single cholesterol molecule is horizontally laid above the graphyne surface within a distance 8.2 Å (less than the cutoff distance of the long-range force). Different initial configurations of the cholesterol molecule are chosen in the simulations to calculate the average adhesive energy between graphyne and the cholesterol molecule. During a long simulation we assume that most stable configurations of the cholesterol-graphyne system will be covered. Figure 4 shows the evolution of adhesive energy between a single cholesterol molecule and 0-, 1-, and 2-graphyne during the simulation time. As the simulation begins, the cholesterol quickly adjusts its configuration to better interact with the graphyne surface which spontaneously changes the adhesive energy between them. The magnitude of the adhesive energy provides a direct measure of the strength of the binding energy between the cholesterol molecule and the graphyne. At equilibrium, 2-graphyne shows an adhesive energy per graphyne atom of 0.043 kcal/mol, greater than 0- (0.019 kcal/mol) and 1-(0.029 kcal/mol) graphyne, which agrees with

the observed strong adhesive strength in graphyne crumpling simulation.<sup>44</sup> Thus, the cholesterol molecule shows the strongest interaction with the 2-graphyne surface and 2-graphyne is anticipated to dislodge more cholesterol molecules from the PCC than 0- and 1-graphyne.

Different from graphene, the porous graphyne might have the capability to uptake cholesterol through its large carbon rings. Thus, it is worthwhile to make a quantitative investigation of penetrating a single cholesterol molecule through porous graphyne. To penetrate the cholesterol molecule into a pore of graphyne, it needs to overcome the strong energy barrier created by the linkers of graphyne. Here, the cholesterol molecule is placed vertically above the graphyne surface at a distance 9 Å with the aromatic ring containing oxygen as head and branch-like –CH<sub>3</sub> group as tail and pulled down towards a specified graphyne pore. The radius of the carbon rings formed by the adjacent linkers (inscribed circle) for 1- and 2- graphyne is estimated as 2.04 Å and 2.84 Å correspondingly. Our simulations show that cholesterol is incapable of penetrating through the carbon ring of 1-graphyne while it can easily pass through the pore of 2-graphyne. Figure 5 shows the evolution of binding energy between the 2-graphyne and the cholesterol molecule as the molecule passes through the 2-graphyne pore. Each snapshot represents the threading through of a different portion of the cholesterol molecule (a), (b), (c) and (d). The aromatic structure of cholesterol at the head makes it different to pass through the graphyne pore which causes a large energy increase as shown in Figure 5(a)-(b). After that, the energy decreases swiftly when the aromatic portion passes through the pore. At point (c), it reaches a local energy minimum of the system which is located in the energy well between the energy barrier (b) and (d) created by the –CH<sub>3</sub> tail of cholesterol. When the cholesterol molecule gets across the pore completely, the binding energy returns to zero. The evolution of the energy barrier for the whole process of cholesterol molecule passing through the graphyne pore implies

that the energetically unfavorable movement of cholesterol molecule through the pores needs to overcome a series of energy barriers. The energy barriers created by the graphyne pore can be conquered by increasing the pressure across the membrane similar to water purification by graphyne.<sup>46, 55</sup> Single cholesterol has little possibility to be unreeved due to the energy barrier at the pore, which in turn suggests that the hybrid structure of graphyne-cholesterol with cholesterol molecule shelved at its local minimum position (c) inside the 2-graphyne pore remains stable. Thus the decorated 2-graphyne with cholesterol molecules inside the pores provides a possible platform to better attract the cholesterol molecules from the protein cluster (see more detail in the following sections). The energy barrier for a single cholesterol molecule penetrating through the graphyne pore is 1900 kcal/mol which is greater than the adhesive energy of the attachment of the cholesterol molecule on the graphyne surface. Through the study of the binding interaction between the cholesterol and graphyne, it can be anticipated that the potential ability of removing cholesterol is related to the number of acetylenic linkers and the hybrid graphyne-cholesterol system might possess a better capability to capture cholesterol than pristine graphyne does.

### **Dependency of cholesterol extraction capability on types of graphyne**

Graphyne offers a better adhesion capability to attach more closely to objects than any other carbon-based materials do.<sup>38</sup> The strong binding ability between graphyne and a single cholesterol molecule in the previous section provides a firm foundation to study the cholesterol extraction efficiency by different types of graphynes in a hybrid system. In what follows, we investigate the dynamic cholesterol extraction process by graphynes and the effect of types of graphynes on the removal efficiency. Figure 6 shows a series of snapshots describing the dynamic process of cholesterol removal by pulling the 0-graphyne through the PCC. When the graphyne sheet approaches to the PCC cluster, the cholesterol molecules begin to move towards

and accumulate on the 0-graphyne surface. The accumulation of the cholesterol molecules on the surface of graphyne and the strong internal entanglement among cholesterol molecules expedite the movement of cholesterol molecules on the surface of graphyne as depicted in Figure 6(a)-(c). Also worthwhile to mention is that the presence of cholesterol molecules roughens the graphyne surface by generating the energy wells on it, which can contribute to the entrapment of cholesterol molecules. From Figure 6(d), it can be noticed that the confined space between two proteins thwarts the continuous collection of cholesterol molecules on the graphyne surface during the pulling process. Two proteins act as the host of cholesterol molecules to hinder their departure from them. However, there is still a larger portion of cholesterol molecules which depart from the PCC during the pulling out of the graphyne sheet as seen in Figure 6(e). The snapshots in Figure 6 demonstrate the fundamental process of how the graphyne is employed to extract the cholesterol molecules from the protein cluster. Figure 7 shows the final results of cholesterol extraction by different types of graphyne. It is noticed that cholesterol molecules can be attached to both sides of the graphyne when removed from the protein cluster. From the side views in Figure 7(b)-(f), we also observe that 2-graphyne deforms more dramatically than 0- and 1- graphyne do because the greater number of linkers makes it more flexible.<sup>44</sup> This flexibility of 2-graphyne can serve an energy well to capture more cholesterol molecules and pull them out together with the graphyne sheet. Comparison of the number of cholesterol molecules extracted by different types of graphyne with the same effective surface area is shown in Figure 8. By showing the nonlinear increase of the number of removed cholesterol molecules from 16, 25 and 53 as the type of graphynes changes from 0 to 2, it implies that the ability of cholesterol extraction by graphyne highly depends on the adhesion between the graphyne and the cholesterol molecules as we have investigated in the previous section and the out-of-plane deformation of

structure. This nonlinear increment relationship is also attributed to the accumulation of cholesterol molecules on the graphyne surface and the wavy surface of graphene, both of which enhance the adhesive capability of the hybrid system of graphyne sheet and cholesterol molecules.

### **Pulling rates of graphyne as a significant factor in cholesterol extraction efficiency**

To determine the effect of pulling rate on the cholesterol extraction from PCC by graphyne, we make a comparison of the removal efficiency of graphyne at different pulling rates for each type of  $\gamma$ -graphyne as well as  $\alpha$ -graphyne,  $\beta$ -graphyne<sup>56</sup>. Figure 8 depicts the number of removed cholesterol molecules by pulling rates of 0.25 Å/ps, 0.5 Å/ps and 1 Å/ps. The dependence of the number of removed cholesterol molecules with pulling velocities could be fitted into equation  $N = ae^{-b/v}$  as shown in Figure 8(c), where  $a$  and  $b$  are coefficient depending on the graphyne types. For 0-graphyne,  $a = 27.9$ ,  $b = -0.34$ ; for 1-graphyne,  $a = 161.0$ ,  $b = -0.93$ ; for 0-graphyne,  $a = 154.4$ ,  $b = -0.42$ . It is noticed that more cholesterol molecules can be extracted from the cluster by a lower pulling rate for all types of  $\gamma$ -graphynes. Under each pulling velocity, a stronger adhesion between graphyne and cholesterol molecules and out-of-plane deformation possesses a larger capability of removing more cholesterol molecules from the cluster. Since the difficulty of the out-of-plane deformation for graphene, the pulling rates we choose here don't have any obvious effect for graphene. The number of removed cholesterol molecules increase from 16 to 18 when decrease the pulling velocity from 0.5 Angstrom/ps to 0.25 Angstrom/ps. The total number of cholesterol molecules in the system is 228 while the 2-graphyne could extract 108 cholesterol molecules from system at pulling velocity 0.25 Angstrom/ps. Compared with 1-graphyne with one triple bond linkers on each edge within 12-atom ring,  $\alpha$ -graphyne has one triple bond linkers could extract more cholesterol molecules due to large deformation of its

18-atom rings with a pulling velocity of 0.5 Å/ps.  $\beta$ -graphyne shows similar extraction efficiency than 1-graphyne. Intuitively, at high pulling speed, the cholesterol molecules close to the graphyne surface do not have enough time to adjust their configuration for better interacting with the graphyne before the graphyne sheet is pulled away. Therefore, there lacks a critical accumulation phase which plays a significant role in determining the efficiency of the removal process. On the other hand, at a lower speed, the cholesterol molecules possess adequate time to adjust their positions on the graphyne surface so as to strongly bind with the graphyne surface, which leads to an easy pull-out process. However, a lower pulling velocity of graphyne sheets needs more computational time. This explains why we choose the default pulling velocity as 0.5 Å/ps to save computation cost while still maintaining the quality of simulation results.

#### **A hybrid graphyne/cholesterol carrier to dislodge the cholesterol molecules**

A variety of appropriate functionalization methods including covalent and non-covalent modifications on the surface of graphene have been reported to enhance its adhesive capability and compatibility with other molecules.<sup>30, 56-62</sup> However the complicated fabrication process for the covalent grafting method together with the instability of non-covalent functionalization of graphene severely hinders its biomedical applications. Different from graphene as mentioned in Section 1, porous 2-graphyne is very suitable to form hybrids with cholesterol molecules by non-covalent functionalization while also possessing outstanding stability. To demonstrate the efficiency of cholesterol extraction from PCC via functionalized 2-graphyne, hybrid structures with high and low densities of cholesterol functionalization are modeled as shown in Figure 9(a) and (b). The cholesterol molecules overcome the energy barrier to enter into the pores of 2-graphyne gradually until reaching the global energy minimum position shown in Figure 5 to make sure that cholesterol molecules retain stable inside the 2-graphyne pores. The stability of

the graphyne-cholesterol hybrid is guaranteed due to the energy barrier which impedes the cholesterol molecules from moving out of the pore in either direction. Figure 9(c) shows the evolution of adhesive energy between a single cholesterol molecule and graphene, and also a single cholesterol molecule with the two hybrid structures. It is noticed that the magnitude of adhesive strength of the hybrid structure with a high density of cholesterol reaches -62 kcal/mol which is higher than that of the structure with a low density of cholesterol -53.7 kcal/mol and pristine 2-graphyne -46.83 kcal/mol, indicating that the strength of adhesion energy between a single cholesterol molecule and functionalized 2-graphyne sheets can be tailored by the extent of the non-covalent binding density of cholesterol molecules. It is also observed that it takes longer simulation time for the single cholesterol to reach its stable configuration on the hybridized 2-graphyne surface than pristine 2-graphyne surface because the single cholesterol molecule needs more time to adjust its position into the shaped wells formed by the functionalized cholesterols. The presence of cholesterol molecules in the 2-graphyne pores endows additional dimensions to the 2-graphyne sheet for interacting with cholesterol molecules.

Will the hybrid structure be more efficient for cholesterol removal than pristine 2-graphyne when pulling it through the PCC? From the simulation results shown in Figure 10(a)-(c), we see that the hybrid structure with a high density of cholesterol molecules, as shown in Figure 9(a), can remove more cholesterol molecules than the low-density structure shown in Figure 9(b). Compared with pristine 2-graphyne, the increased number of removed cholesterol molecules indicates that the functionalized hybrid structure emerges as a more powerful tool to disentangle and extract the cholesterol molecules from the PCC, as shown in Figure 10(c). It is also noticed from Figure 10(a) and (b), that during the pulling process the cholesterol molecules in the pores always retain their position and stay in the 2-graphyne pore, implying that the energy to overcome

the pull-out barrier of a single cholesterol molecule from the graphene pore is larger than the energy to move it freely on the surface of hybrid structure. Our findings demonstrate that the proposed hybrid 2-graphyne structure possesses extraordinary binding properties to attract cholesterol molecules, which can serve as a platform for the medical application of graphyne-based hybrid structures.

### **Concluding remarks**

In summary, we have performed molecular dynamics simulation to investigate how to pull cholesterol molecules from a protein cluster by graphyne sheets. We first demonstrated the adhesive strength between the graphyne and single cholesterol which laid the foundation for pulling the cholesterol molecules out from the protein cluster. With strong per-atom interaction, the graphyne can fully interact with local cholesterols and attract them to its surface when it passes through the PCC. Our simulation results suggest that the number of acetylenic linkers ( $N$ ) of the graphyne is the strongest indicator of the efficiency for extracting cholesterol molecules from the system of interest. The out-of-plane deformation of graphyne with more linkers makes it easier to carry the cholesterols out. The ability of cholesterol extraction by graphyne depends on both the adhesion between the graphyne and cholesterol molecules and the irregular morphology of graphyne with the increase of the number of the linkers. The extraction efficiency is also influenced by the graphyne pulling rate through the protein cluster, with a slower pulling rate able to remove more cholesterol molecules no matter what type of graphyne it is. We also designed a stable hybrid graphyne/cholesterol carrier by placing the cholesterol molecule into the graphyne pores. This hybrid shows an intense adhesive strength able to attract more cholesterol molecules and remove them from the protein cluster compared with the pristine graphynes.

These fundamental findings provide a promising guidance for designing novel carbon-based devices for biomedical purposes.

### **Acknowledgements**

The authors acknowledge support from the National Science Foundation (Grant. No. CMMI-1306065) and University of Georgia (UGA) start-up fund. The facility support for modeling and simulations from the UGA Advanced Computing Resource Center is greatly appreciated.

### **Additional information**

Competing financial interests: The authors declare no competing financial interests.

## References

1. P. L. Yeagle, *Biochimica et biophysica acta*, 1985, 822, 267-287.
2. B. Hissa, B. Pontes, P. M. Roma, A. P. Alves, C. D. Rocha, T. M. Valverde, P. H. Aguiar, F. P. Almeida, A. J. Guimaraes, C. Guatimosim, A. M. Silva, M. C. Fernandes, N. W. Andrews, N. B. Viana, O. N. Mesquita, U. Agero and L. O. Andrade, *Plos One*, 2013, 8, e82988.
3. G. Khelashvili and D. Harries, *J. Phys. Chem. B*, 2013, 117, 2411-2421.
4. N. Khatibzadeh, S. Gupta, B. Farrell, W. E. Brownell and B. Anvari, *Soft Matter*, 2012, 8, 8350-8360.
5. J. P. Incardona and S. Eaton, *Curr Opin Cell Biol*, 2000, 12, 193-203.
6. M. Zocher, C. Zhang, S. G. Rasmussen, B. K. Kobilka and D. J. Muller, *P Natl Acad Sci USA*, 2012, 109, E3463-3472.
7. H. J. Kaiser, A. Orłowski, T. Rog, T. K. Nyholm, W. Chai, T. Feizi, D. Lingwood, I. Vattulainen and K. Simons, *P Natl Acad Sci USA*, 2011, 108, 16628-16633.
8. A. Ivankin, I. Kuzmenko and D. Gidalevitz, *Phys. Rev. Lett.*, 2012, 108, 238103.
9. B. Hissa, J. G. Duarte, L. F. Kelles, F. P. Santos, H. L. del Puerto, P. H. Gazzinelli-Guimaraes, A. M. de Paula, U. Agero, O. N. Mesquita, C. Guatimosim, E. Chiari and L. O. Andrade, *PLoS neglected tropical diseases*, 2012, 6, e1583.
10. M. Alwarawrah, J. Dai and J. Huang, *J. Phys. Chem. B*, 2010, 114, 7516-7523.
11. W. F. Bennett, J. L. MacCallum and D. P. Tieleman, *J. Am. Chem. Soc.*, 2009, 131, 1972-1978.
12. D. J. Gordon, J. L. Probstfield, R. J. Garrison, J. D. Neaton, W. P. Castelli, J. D. Knoke, D. R. Jacobs, Jr., S. Bangdiwala and H. A. Tyroler, *Circulation*, 1989, 79, 8-15.
13. J. L. Goldstein and M. S. Brown, *Science*, 2001, 292, 1310-1312.
14. F. R. Maxfield and I. Tabas, *Nature*, 2005, 438, 612-621.
15. L. F. Van Gaal, I. L. Mertens and C. E. De Block, *Nature*, 2006, 444, 875-880.
16. J. Genest, *J. Inherit. Metab. Dis.*, 2003, 26, 267-287.
17. P. Amarenco, J. Labreuche and P. J. Touboul, *Atherosclerosis*, 2008, 196, 489-496.
18. M. J. Chapman, *Pharmacol. Ther.*, 2006, 111, 893-908.
19. C. A. Mirkin, C. S. Thaxton, D. A. Giljohann and W. Daniel, Google Patents, 2012.
20. T. Kalburcu, N. Ozturk, N. Tuzmen, S. Akgol and A. Denizli, *J. Ind. Eng. Chem.*, 2014, 20, 153-159.
21. H. S. Lye, G. Rusul and M. T. Liong, *J. Dairy Sci.*, 2010, 93, 1383-1392.
22. H. S. Lye, A. A. Karim, G. Rusul and M. T. Liong, *J. Dairy Sci.*, 2011, 94, 4820-4830.
23. C. A. Lopez, A. H. de Vries and S. J. Marrink, *PLoS computational biology*, 2011, 7, e1002020.
24. C. A. Lopez, A. H. de Vries and S. J. Marrink, *Sci. Rep.*, 2013, 3, 2071.
25. Z. Gburski, K. Gorny and P. Raczynski, *Solid State Commun.*, 2010, 150, 415-418.
26. I. V. Pavlidis, M. Patila, U. T. Bornscheuer, D. Gournis and H. Stamatis, *Trends Biotechnol.*, 2014, 32, 312-320.
27. D. Bitounis, H. Ali-Boucetta, B. H. Hong, D. H. Min and K. Kostarelos, *Adv. Mater.*, 2013, 25, 2258-2268.
28. K. V. Krishna, C. Menard-Moyon, S. Verma and A. Bianco, *Nanomedicine*, 2013, 8, 1669-1688.
29. M. Hirtz, A. Oikonomou, T. Georgiou, H. Fuchs and A. Vijayaraghavan, *Nat Commun*, 2013, 4, 2591.
30. L. Zhang, X. Zeng and X. Wang, *Sci Rep*, 2013, 3, 3162.
31. Y. Yang, A. Asiri, Z. Tang, D. Du and Y. Lin, *Materials Today*, 2013, 16, 365-373.
32. Y. Li, H. Yuan, A. von dem Bussche, M. Creighton, R. H. Hurt, A. B. Kane and H. Gao, *Proc Natl Acad Sci U S A*, 2013, 110, 12295-12300.
33. O. Akhavan and E. Ghaderi, *ACS Nano*, 2010, 4, 5731-5736.

34. S. Liu, T. H. Zeng, M. Hofmann, E. Burcombe, J. Wei, R. Jiang, J. Kong and Y. Chen, *ACS Nano*, 2011, 5, 6971-6980.
35. Y. Tu, M. Lv, P. Xiu, T. Huynh, M. Zhang, M. Castelli, Z. Liu, Q. Huang, C. Fan, H. Fang and R. Zhou, *Nat. Nanotechnol.*, 2013, 8, 594-601.
36. G. Li, Y. Li, H. Liu, Y. Guo, Y. Li and D. Zhu, *Chem Commun (Camb)*, 2010, 46, 3256-3258.
37. M. M. Haley, S. C. Brand and J. J. Pak, *Angewandte Chemie International Edition in English*, 1997, 36, 836-838.
38. S. W. Cranford and M. J. Buehler, *Carbon*, 2011, 49, 4111-4121.
39. J. Zhao, N. Wei, Z. Fan, J. Jiang and R. Timon, *Nanotechnology*, 2013, 24, 095702.
40. K. Srinivasu and S. K. Ghosh, *J. Phys. Chem. C*, 2012, 116, 5951-5956.
41. J. Kang, J. B. Li, F. M. Wu, S. S. Li and J. B. Xia, *J. Phys. Chem. C*, 2011, 115, 20466-20470.
42. C. Albarran-Diego, G. Munoz, T. Ferrer-Blasco, S. Garcia-Lazaro and L. Belda-Salmeron, *J. Refract. Surg.*, 2012, 28, 380-386.
43. H. J. Hwang, J. Koo, M. Park, N. Park, Y. Kwon and H. Lee, *J. Phys. Chem. C*, 2013, 117, 6919-6923.
44. M. Becton, L. Zhang and X. Wang, *Phys. Chem. Chem. Phys.*, 2014, 16, 18233-18240.
45. J. Kou, X. Zhou, Y. Chen, H. Lu, F. Wu and J. Fan, *J. Chem. Phys.*, 2013, 139, 064705.
46. S. Lin and M. J. Buehler, *Nanoscale*, 2013, 5, 11801-11807.
47. J. Zheng, X. Zhao, Y. Zhao and X. Gao, *Sci Rep*, 2013, 3, 1271.
48. B. R. Brooks, R. E. Bruccoleri, B. D. Olafson, D. J. States, S. Swaminathan and M. Karplus, *J Comput Chem*, 1983, 4, 187-217.
49. A. D. Mackerell, D. Bashford, M. Bellott, R. L. Dunbrack, J. D. Evanseck, M. J. Field, S. Fischer, J. Gao, H. Guo, S. Ha, D. Joseph-McCarthy, L. Kuchnir, K. Kuczera, F. T. Lau, C. Mattos, S. Michnick, T. Ngo, D. T. Nguyen, B. Prodhom, W. E. Reiher, B. Roux, M. Schlenkrich, J. C. Smith, R. Stote, J. Straub, M. Watanabe, J. Wiorkiewicz-Kuczera, D. Yin and M. Karplus, *J. Phys. Chem. B*, 1998, 102, 3586-3616.
50. A. D. Mackerell, Jr., M. Feig and C. L. Brooks, 3rd, *J Comput Chem*, 2004, 25, 1400-1415.
51. G. Zygmunt, G. Krzysztof, R. Przemysław and D. Aleksander, in *Carbon Nanotubes - Growth and Applications*, ed. M. Naraghi, InTech, 2011, ch. 20, p. 493.
52. J. Hénin and C. Chipot, *Chemical Physics Letters*, 2006, 425, 329-335.
53. H. J. C. Berendsen, J. P. M. Postma, W. F. Vangunsteren, A. Dinola and J. R. Haak, *J. Chem. Phys.*, 1984, 81, 3684-3690.
54. D. Bashford and D. A. Case, *Annu. Rev. Phys. Chem.*, 2000, 51, 129-152.
55. J. Kou, X. Zhou, H. Lu, F. Wu and J. Fan, *Nanoscale*, 2014, 6, 1865-1870.
56. Y. Zhang, Q. Pei and C. Wang, *Applied Physics Letters*, 2012, 101, 081909.
57. C. Zhang and T. X. Liu, *Chinese Sci Bull*, 2012, 57, 3010-3021.
58. L. Zhang and X. Wang, *Phys Chem Chem Phys*, 2014, 16, 2981-2988.
59. M. Becton, L. Y. Zhang and X. Q. Wang, *Chem. Phys. Lett.*, 2013, 584, 135-141.
60. L. Bo, A. B. Julia, V. D. Sergey, W. Xu, Z. Hongwei and Z. Kun, *J. Phys. D: Appl. Phys.*, 2013, 46, 305302.
61. B. Liu, C. D. Reddy, J. W. Jiang, J. A. Baimova, S. V. Dmitriev, A. A. Nazarov and K. Zhou, *Applied Physics Letters*, 2012, 101, 211909.
62. L. Zhang and X. Wang, *Journal of Applied Physics*, 2014, 115, 194306.

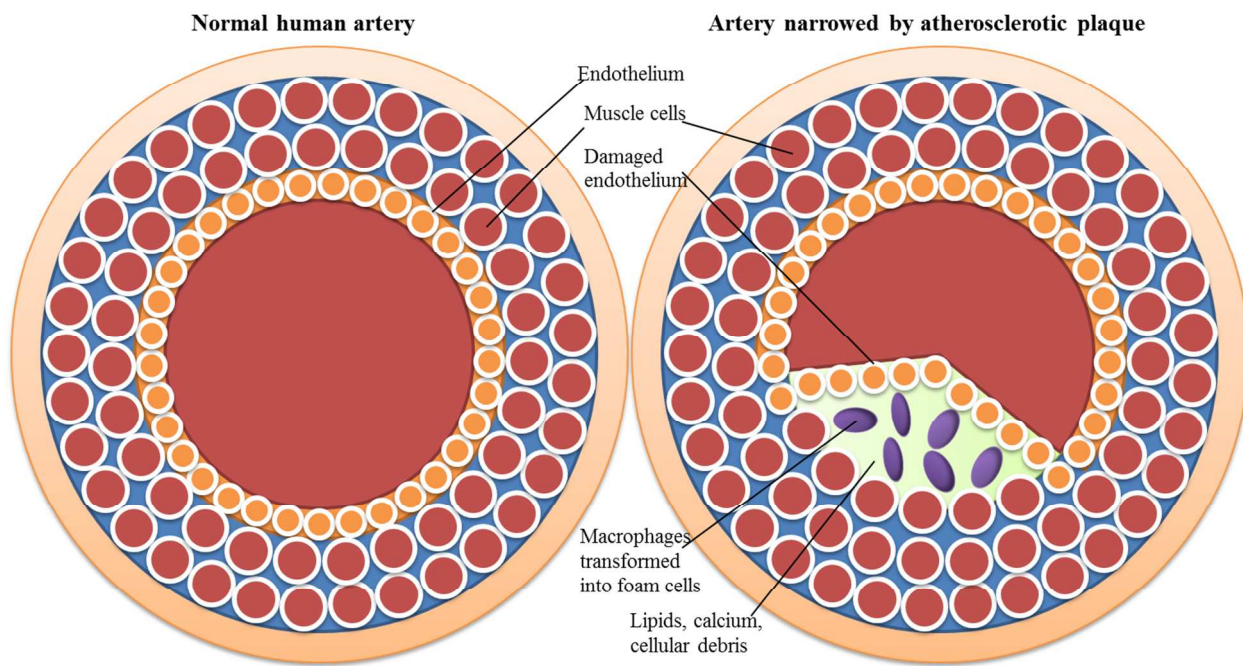


Figure 1. Structure of human artery before and after Atherosclerosis

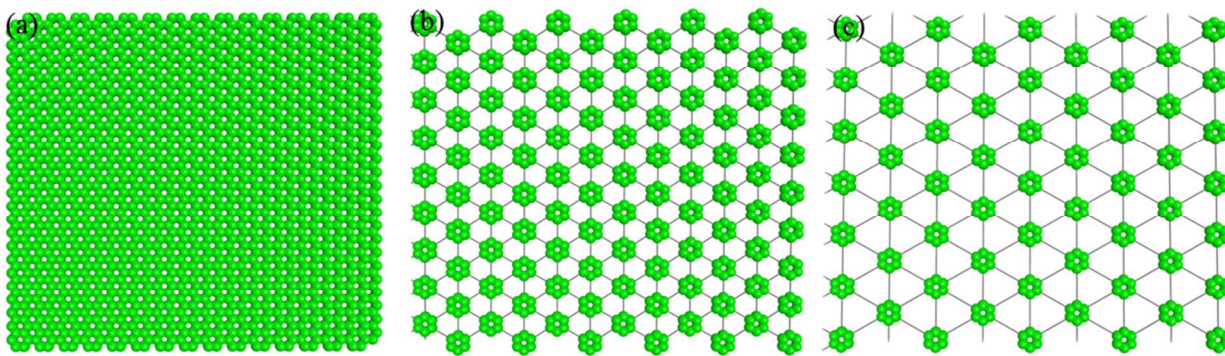


Figure 2. Atomistic structure of graphynes: (a) 0-graphyne. (b) 1-graphyne. (c) 2-graphyne. The aromatic ring is highlighted in green. The dangling carbon atoms at the edges of the graphynes are terminated by hydrogen atoms.

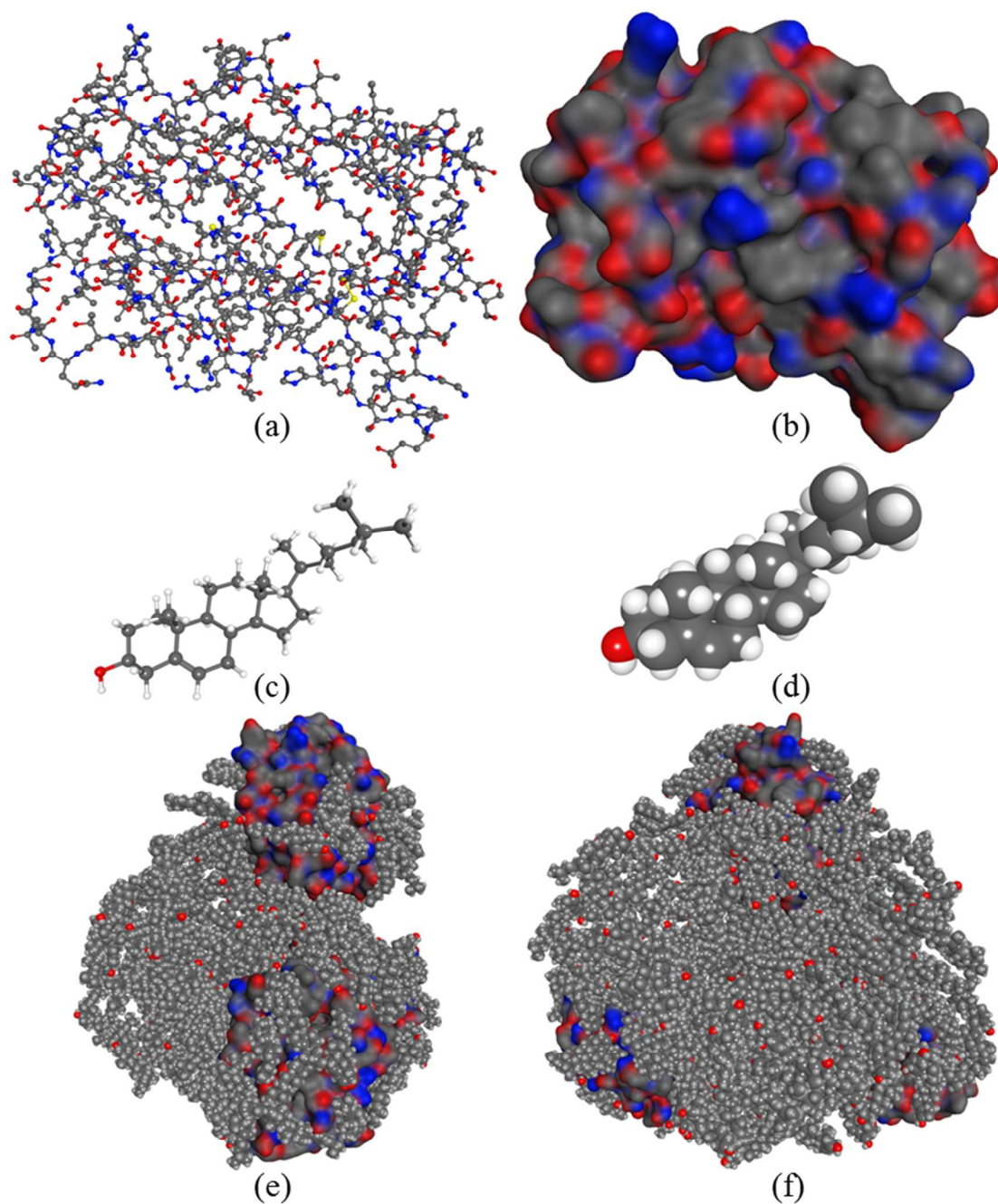


Figure 3. (a) Full atomistic view of 1LQV protein. (b) Surface view of 1LQV protein based on the element color. (c) Full atomistic view of a single cholesterol molecule. (d) Bead view of a single cholesterol molecule. (e) Model of anfractuous protein-cholesterol Cluster (PCC). (f) Side view of PCC

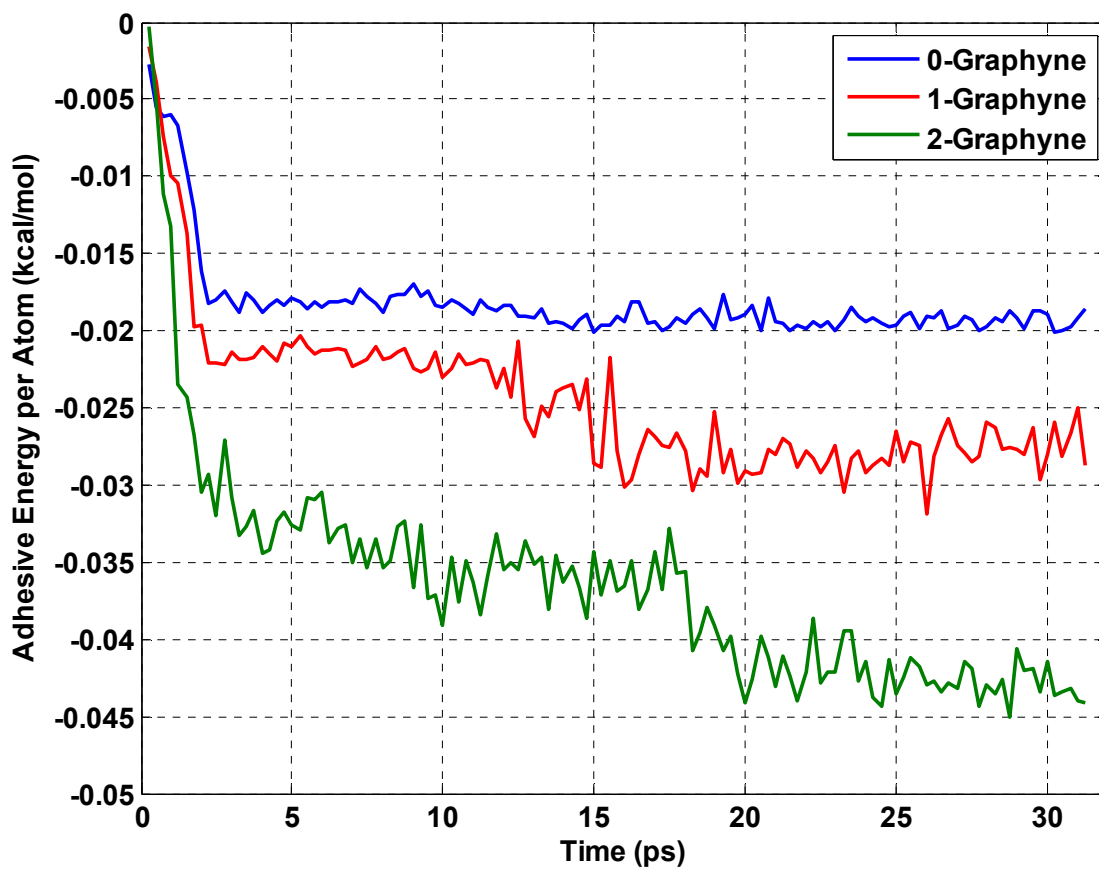


Figure 4. Evolution of adhesive energy of a single cholesterol molecule on *N*-graphyne with simulation time

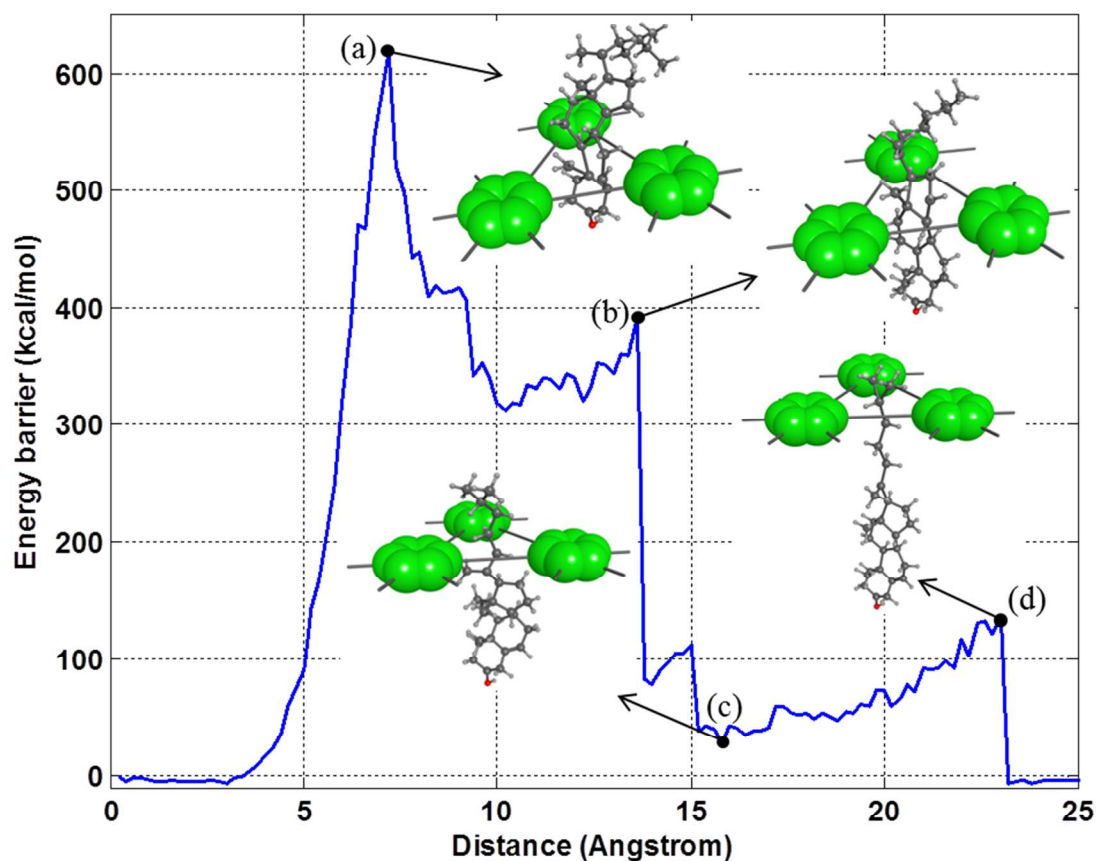


Figure 5. Evolution of energy changes for a single cholesterol molecule as it passes through the 2-grahyne pore. (a) Snapshot for the moment the first aromatic ring at the head position of cholesterol molecule passes through the pore. (b) Snapshot for the moment the second aromatic ring at the head position of cholesterol molecule passes through the pore. (c) Snapshot for the moment an energy minimum reaches. (d) Snapshot for the moment  $-CH_3$  branch-like group in cholesterol molecule passes through the pore.

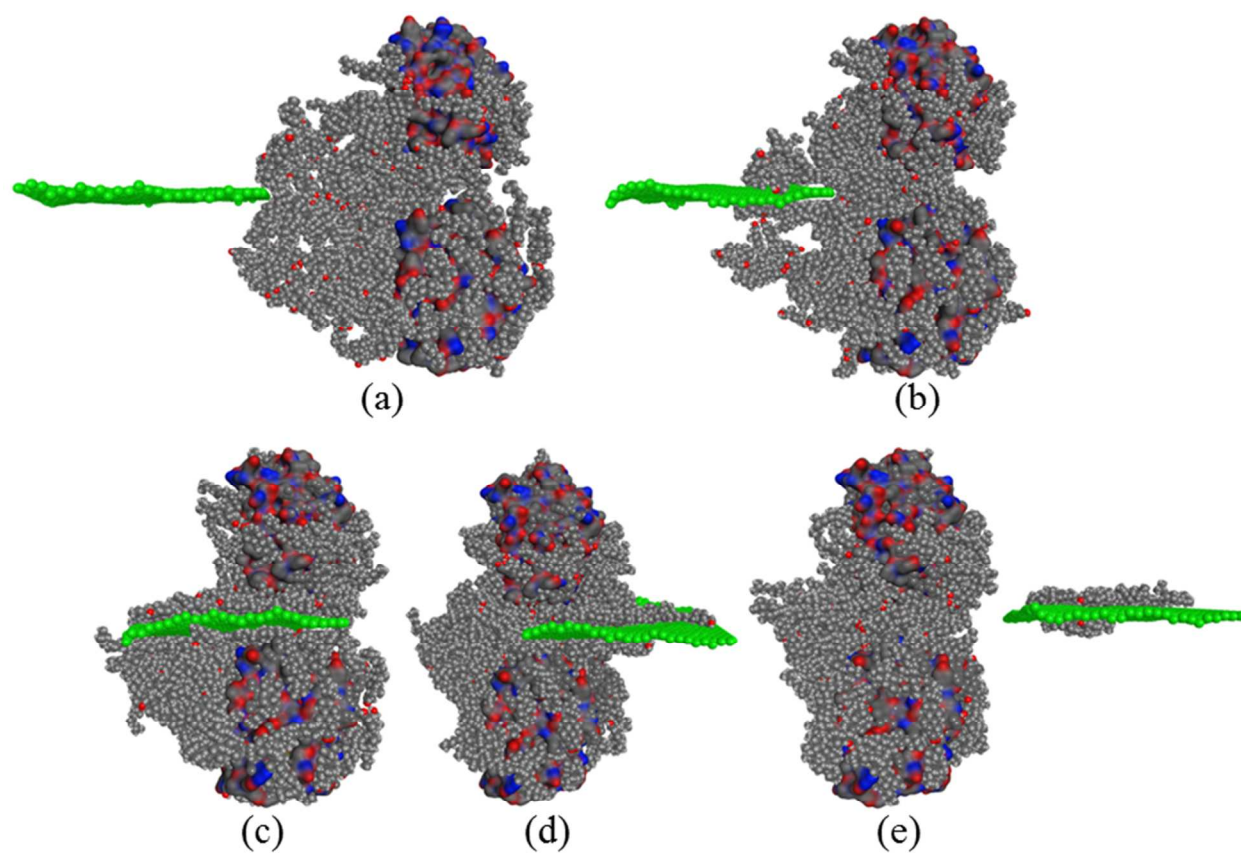


Figure 6. A series of snapshots describe the dynamic pulling process for removing cholesterol from the PCC by using 0-graphyne. 0-graphyne is shown in green.

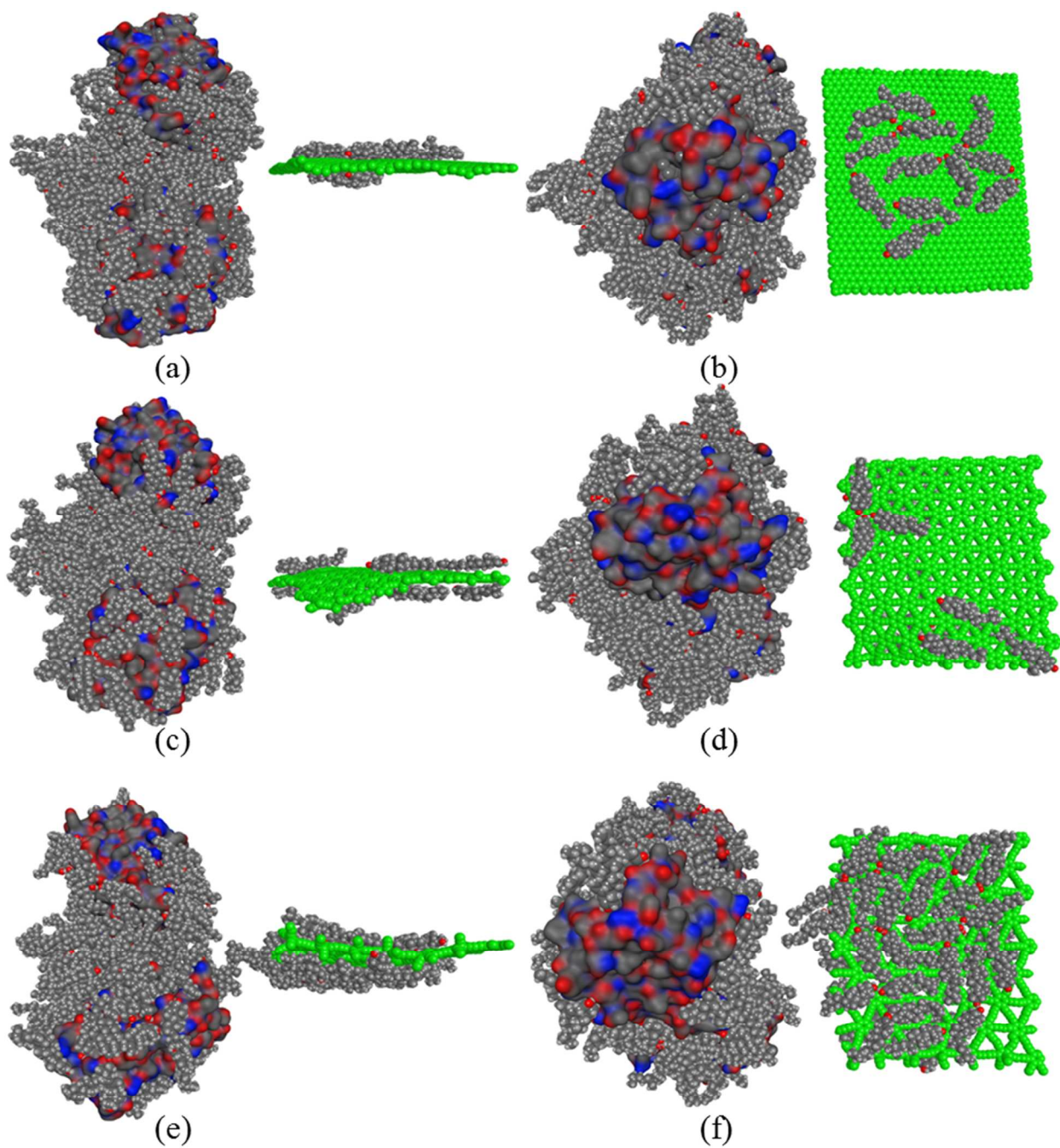


Figure 7. Final snapshots of simulations with 0-graphyne (a, b), 1-graphyne (c, d), 2-graphyne (e, f) respectively. (a)-(c)-(e) Side view. (b)-(d)-(f) Top view.

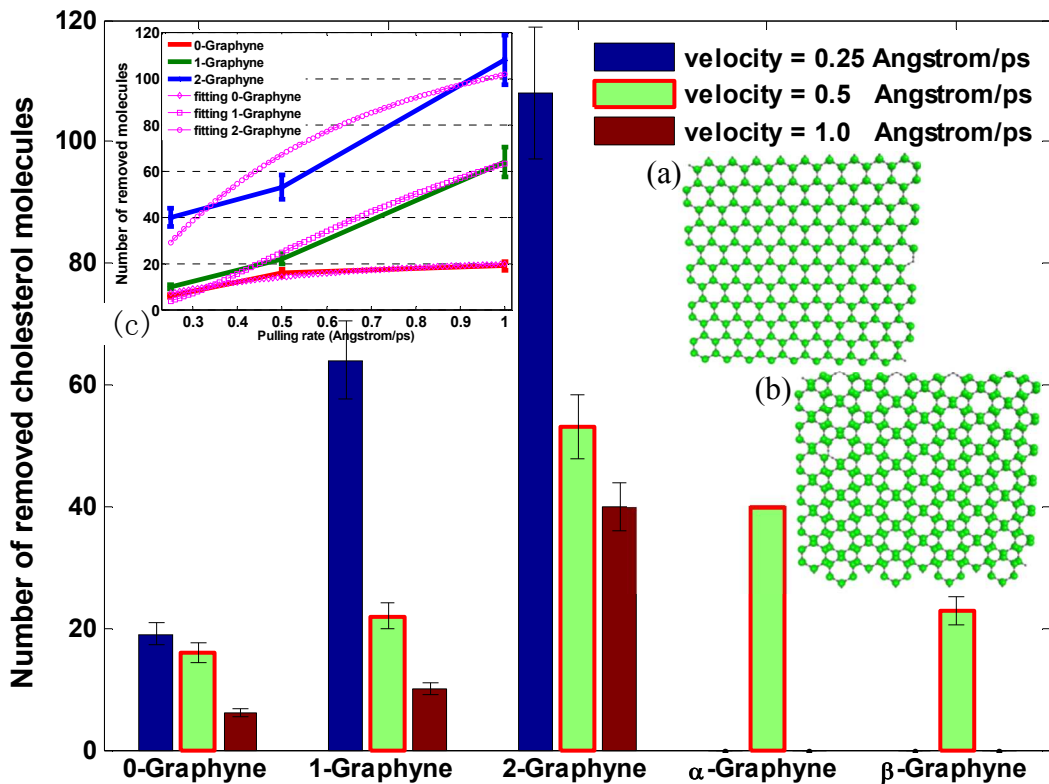


Figure 8. Number of removed cholesterol molecules from the protein cluster with a variety of pulling rates for 0-, 1-, 2-graphyne as well as  $\alpha$ - (a),  $\beta$ -graphyne (b). (c) shows the explicit relationship between the number of removed cholesterol molecules and the pulling velocities for three different graphynes.

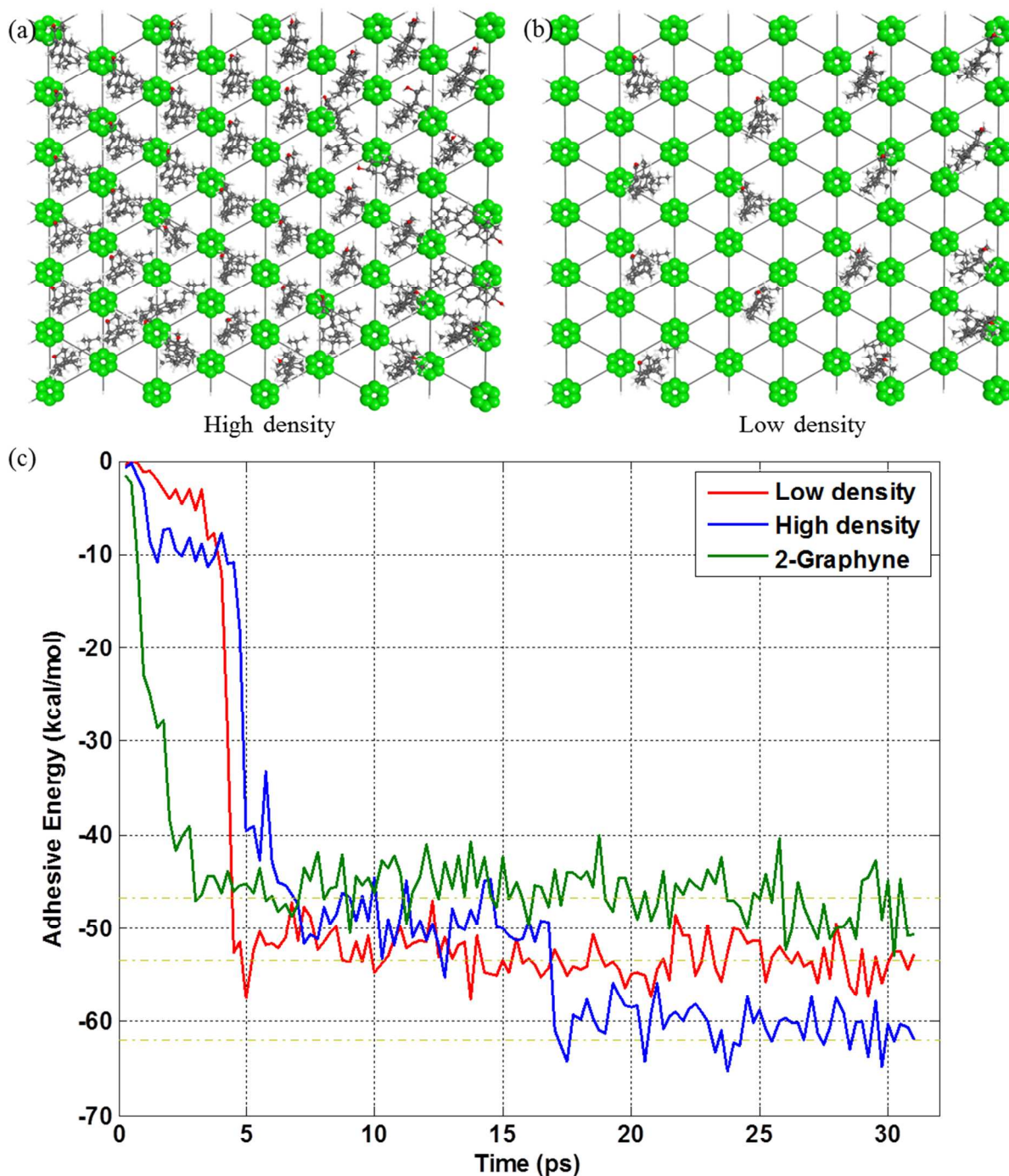


Figure 9. A hybrid graphyne/cholesterol carrier with high (a) and low density (b) of cholesterol's decoration. (c) Evolution of adhesive energy of a single cholesterol molecule on the surface of 2-graphyne, hybrid structure (a) and hybrid structure (b) separately. The brown dash line depicts the averaged energy at equilibrium state.

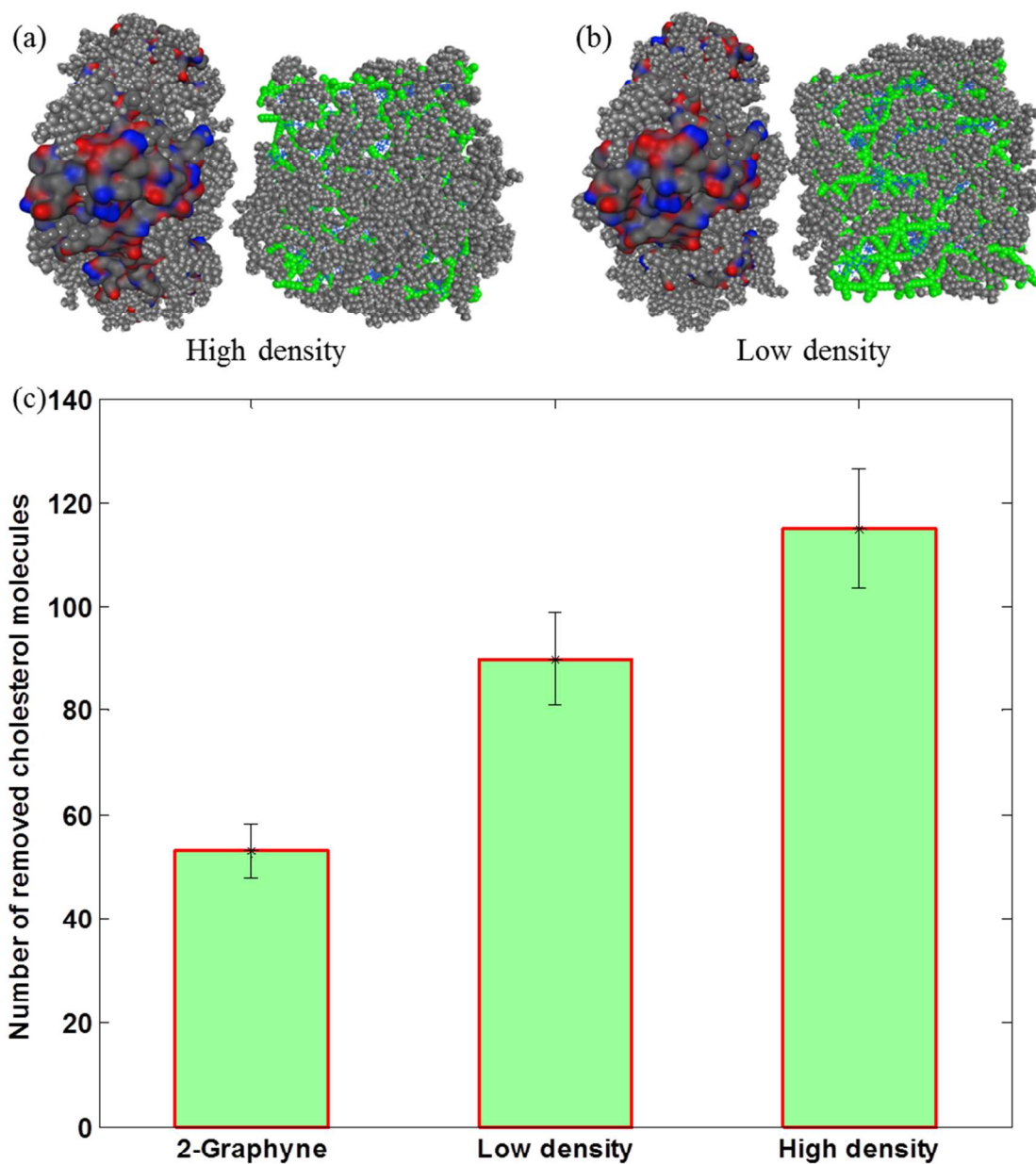


Figure 10 (a) Final snapshot of simulations for functionalized 2-graphyne with high density of cholesterol molecules. (b) Final snapshot of simulations for functionalized 2-graphyne with low density of cholesterol molecules. The cholesterol molecules used to functionalize 2-graphyne are shown in blue color to make a distinction to the cholesterol molecules in the PCC. (c) Number of removed cholesterol molecules from PCC with pristine 2-graphyne, hybrid 2-graphyne with high density of functionalization, hybrid 2-graphyne with low density of functionalization.